

## Oxide Nanointerface Engineering for Microwave Electronic Devices

K.Y. Constantinian<sup>1</sup>, G.A. Ovsyannikov<sup>1</sup>, A.V. Shadrin<sup>1</sup>, Yu.V. Kislinskii<sup>1</sup>,  
A.M. Petrzhek<sup>1</sup>, A.V. Zaitsev<sup>1</sup>, J. Mygind<sup>2</sup> and D. Winkler<sup>3</sup>

<sup>1</sup> Kotelnikov Institute of Radio Engineering and Electronics RAS, Moscow, Russia

<sup>2</sup> Department of Physics, Technical University of Denmark, Lyngby, Denmark

<sup>3</sup> Chalmers University of Technology, Gothenburg, Sweden

We report on experimental studies of electron transport, microwave properties and noise in the multilayer hybrid superconducting heterostructures with magneto-active interlayer. The base electrode was copper oxide superconductor used for forming the interface with magnetic material made from either cuprate antiferromagnetic CaSrCuO, or underdoped LaMnO, or Ca doped manganite. The upper electrode was Au/Nb bilayer. In the case of antiferromagnetic CaSrCuO interlayer (with thickness  $12 \div 50$  nm) the  $I$ - $V$  curves demonstrated good fit to RSJ-model showing critical frequency  $f_C$  of order 100 GHz at  $T=4.2$  K. At the same time, non-integer Shapiro steps were observed along with the sub-harmonic detector response. The second harmonic of the current-phase relation of order  $10 \div 20\%$  of the first one was evaluated via measurements of integer and half-integer Shapiro steps.

### 1. Introduction

Coexistence of superconducting and magnetic ordering in solids is of great interest for fundamental physics and electronic applications. The exchange mechanism of ferromagnetic ordering tends to align spins of superconducting pairs in the same direction preventing singlet pairing [1-2]. At the interfaces between superconducting (S) and magnetic matter (M), however, the superconducting and magnetic correlations may interact due to the proximity effect (penetration of superconducting correlations into magnetic matter) resulting in interplay between superconducting and magnetic ordering, and novel physical phenomena may appear. However, up to now most of the activity was devoted to investigations of heterostructures where M-interlayer is a ferromagnetic (F). However, much less attention was paid to superconducting structures with M-interlayer having AF- ordering. Recently L. Gor'kov and V. Kresin [3] assumed a model (G-K model) of the S/AF/S structure where an AF interlayer consists of F-layers with antiparallel magnetizations and aligned perpendicular to the surface of the S-electrodes. The G-K model predicts existence of critical current like in S/N/S structures with spacing between S electrodes larger than the coherence length  $\xi_N$  in normal metal N. The G-K model also predicts that a minor change in canting of magnetic moments in the F-layers caused, say, by external magnetic field  $H$  will reduce sharply the critical current  $I_c$ . Theoretical investigation of a S/M/S structure with M-interlayer composed of  $N$  F-layers each one with a thickness exceeding the atomic-scale was carried out also in [4] by A.V. Zaitsev. The orientation of the F-layer magnetizations in the latter model was parallel to the S/M interface and it was shown that for AF- ordering the long-range proximity effect takes place. Experimental observation of the Josephson effect in S/AF/S structures Nb/Cu/FeMn/Nb has been demonstrated in [5], where AF- interlayer was  $\gamma$ -Fe<sub>50</sub>Mn<sub>50</sub> alloy. If instead of using a polycrystalline metallic AF-material one would substitute it by an array of F-layers with alternating directions of magnetization, according to the G-K model the dependence  $I_c(H)$  should then exhibit rapid oscillations. Recently experimental observations of such oscillations and the critical current dependence on M-interlayer thickness have been shown [6-8].

In order to observe long-range proximity effect in superconducting structure with M-interlayer, a transparent S/M interface is needed. This is also why in-depth investigations of such interfaces composed of the superconducting and antiferromagnetic cuprate materials are highly relevant. At the same time mutual influence of antiferromagnetism and the d-wave superconductivity at S/M interfaces in Josephson junctions also is necessary to unveil. In this paper we report on the experimental studies of dc and microwave current transport through S/M interfaces realized in hybrid Nb/Au/M/YBa<sub>2</sub>Cu<sub>3</sub>O<sub>7- $\delta$</sub>  mesa heterostructures (MHS) with the in-plane size  $L$  varied from 10 to 50  $\mu$ m. Here Nb is a conventional s-wave superconductor (S'), YBa<sub>2</sub>Cu<sub>3</sub>O<sub>7- $\delta$</sub>  (YBCO) is a cuprate superconductor with the dominating d-wave order parameter ( $S_d$ ), and Au is a normal metal (N). The M-interlayer is either the Ca<sub>1- $x$</sub> Sr <sub>$x$</sub> CuO<sub>2</sub> (CSCO) ( $x=0.15$  or  $0.5$ ) which is a quasi-two-dimensional Heisenberg antiferromagnetic cuprate, or underdoped manganite LaMnO<sub>3</sub>, or doped ferromagnetic half-metal La<sub>1- $y$</sub> Ca <sub>$y$</sub> MnO<sub>3</sub> manganite.

## 2. Experimental technique

The double-layer epitaxial thin film structures M/YBCO were grown *in-situ* by pulsed laser ablation on (110) NdGaO<sub>3</sub> (NGO) substrates. The c-axis of the M/ S<sub>d</sub> heterostructures is perpendicular to the substrate surface. Typically, the  $d=5\div 100$  nm thick M-films were deposited on the top of 150 nm thick YBCO films. The Ca<sub>1-x</sub>Sr<sub>x</sub>CuO films ( $x=0.15$  and  $x=0.5$ ) were used as M-interlayers, and La<sub>1-y</sub>Ca<sub>y</sub>MnO<sub>3</sub> ( $y=0$  and  $y=0.3$ ) as possible candidates for magnetic interlayer as recommended in [3]. The M/YBCO heterostructures were covered *in-situ* by a 10÷20 nm thick Au film and afterwards, a 200 nm thick Nb film was deposited *ex-situ* by dc-magnetron sputtering in an Ar atmosphere. In order to fabricate Nb/Au/M/YBCO mesas we utilize optical photolithography, reactive plasma etching, and Ar ion-milling techniques. A SiO<sub>2</sub> protective layer was deposited by RF-magnetron sputtering. An additional 200 nm thick Nb/Au bilayer film was deposited on the top of the MHS and patterned in order to form the superconducting wiring. The square S'/N/M/S<sub>d</sub> MHS with areas  $S=L^2$  from 10×10 μm<sup>2</sup> up to 50×50 μm<sup>2</sup> were fabricated (see Fig. 1).

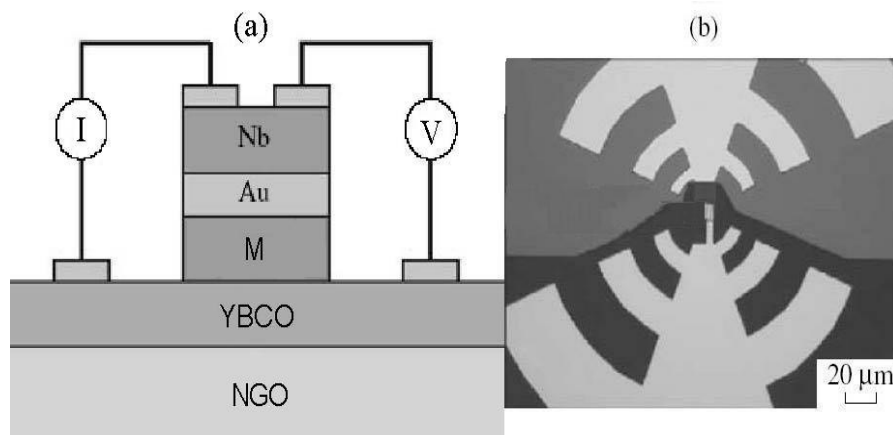


Fig. 1. (a) - The cross section of the MHS. The layers thicknesses are: YBCO –150 nm, M-interlayer 5÷100 nm, Au - 10÷20 nm, Nb – 200 nm. (b) - Top view of MHS incorporated with log periodic antenna.

For comparison, a similar fabrication procedure was used for structuring of the MHS without M-interlayer [9]. Direct Nb deposition on top of the YBCO film results in formation of Nb/YBCO interface with very high resistance ( $\sim 1 \Omega \cdot \text{cm}^2$ ) due to the Nb film oxidation. Thus, if the Au layer is locally damaged because of the finite surface roughness of the M/S<sub>d</sub> interface then niobium oxide prevents pinholes formation.

## 3. Results and discussion

The resistance of MHS is  $R=R_{YBCO}+R_{MY}+R'_M+R_b+R_{Nb/Au}+R_{Nb}+R_{Au}$ , where  $R_{YBCO}$  comes from YBCO electrode,  $R_{MY}$  is the M/YBCO interface resistance,  $R'_M$  is the resistance of the M-interlayer,  $R_b$  is the Au/M interface barrier resistance, and the resistances  $R_{Nb}$  and  $R_{Au}$  for Nb electrode and Au film, respectively. The contribution of thin Au film can be neglected [9]. Fig.2. shows temperature dependences of MHS resistance and the CSCO layer. Independently measured characteristic resistivity of the Nb/Au interface ( $\sim 10^{-11} \Omega \cdot \text{cm}^2$ ) [9] results in  $R_{Nb/Au} \sim 1 \mu\Omega$  - a negligibly small contribution to total resistance of MHS. Taking into account the epitaxial growth of the CSCO/YBCO structure and similar parameters of the crystal structure of contacting materials, one can assume that interface resistance  $R_{MY}$  is small compared to the resistance  $R_b$  of the Au/CSCO interface, for which the difference between Fermi velocities of Au and the CSCO is significant [9]. The thickness dependencies of specific resistance  $R_N S$  of MHS is given in Fig.3. Although the structures with manganite M-interlayer had no critical current, the most of samples with AF CSCO interlayer demonstrated Josephson effect and symmetric RSJ-type [10]  $I$ - $V$  curve without excess current had  $I_C R_N \sim 200 \mu\text{V}$  at  $T=4.2$  K. All junctions had dimensions  $L < \lambda_J$ , where  $\lambda_J$  is Josephson penetration depth, and McCumber parameter  $\beta_c=1\div 3$ . Thickness dependence of critical current density  $j_c(d)$  for S/AF/S junction with  $x=0.5$  in CSCO interlayer is shown in Fig. 4.

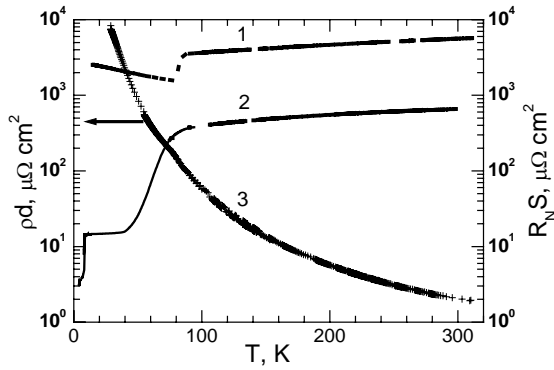


Fig.2. Temperature dependences of junction resistance: (1)  $d=20$  nm,  $S=10 \times 10 \mu\text{m}^2$ , (2)  $d=40$  nm,  $S=50 \times 50 \mu\text{m}^2$  and (3) resistance  $\rho d/S$  of a bare CSCO film with  $x=0.5$ ,  $d=40$  nm,  $S=50 \times 50 \mu\text{m}^2$  deposited on NGO substrate.

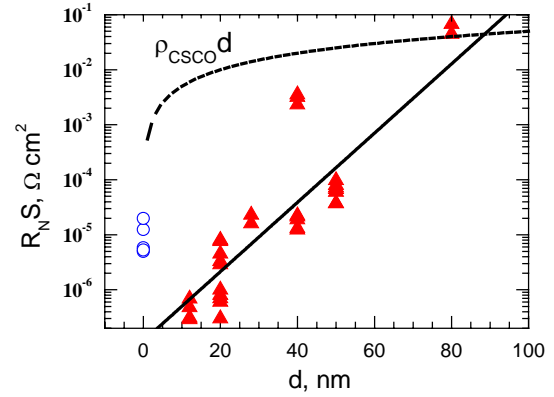


Fig.3. Thickness dependences of specific resistance  $R_N S$  for CSCO with  $x=0.5$ . Bold line corresponds to  $\xi_{AF} = 7 \pm 1$  nm. Open circles - for junctions without AF interlayer. Dash line is calculated resistance for bare CSCO AF layer.

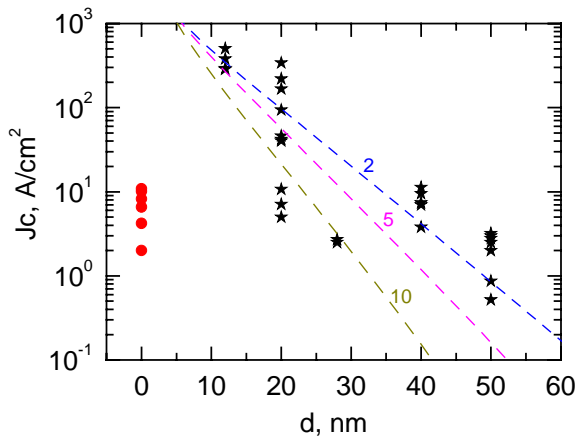


Fig. 4. Thickness dependences of critical current density for junctions with (and without  $d=0$ ) AF interlayer. Dashes are theoretical dependences for S/AF/S junctions with different intensity of exchange field  $h$  (numbers) in F.

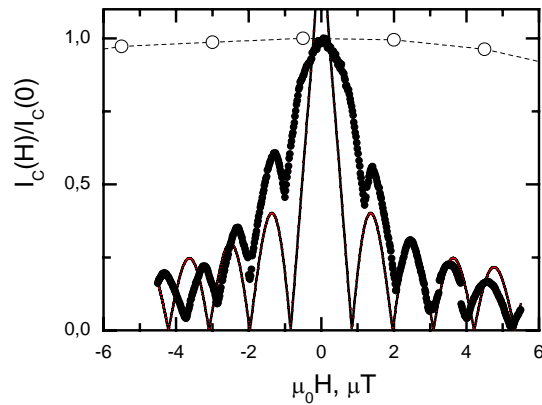


Fig.5. Magnetic-field dependence  $I_C(H)$  for structures with  $L = 50 \mu\text{m}$ . With AF interlayer - black points, thin line is theory [3]. A central part of  $I_C(H)$  for a structure without AF layer - open circles.

Theoretical dependences  $j_c(d)$  are also plotted for a model of S/AF/S junction with a magnetic interlayer consisting from  $N=20$  ferromagnetic layers with opposite magnetization. The best fit gives the theoretical dependence for the exchange field  $h=H_{ex}/\pi kT=5$  plotted for the case when coherence depth in AF  $\xi_{AF}=10$  nm. Fig.5 demonstrate magnetic-field dependence  $I_C(H)$  for junctions with the same dimensions,  $L = 50$  nm, one with, and other without AF interlayer. The calculation of  $I_C(H)$  by [3] for S/AF/S junctions shows huge increase in sensitivity to applied  $H$ -field in comparison with structures without AF interlayer.

The dominant d-wave symmetry of the  $S_d$  electrode results in a non-sinusoidal CPR for MHS with c-axis oriented YBCO:  $I_s(\varphi) = I_{c1} \sin \varphi + I_{c2} \sin 2\varphi + \dots$ . The values of the second harmonics of the CPR were defined from measurements of Shapiro steps at  $f_c = 36 \div 120$  GHz. All MHS demonstrated Shapiro steps with strong modulation as a function of the microwave power (inset to Fig. 6). The modulation of the amplitudes of the Shapiro steps vs. applied microwave power (Fig. 6) confirms the Josephson effect origin of the superconducting current. Less than 20% difference has been observed between the critical frequency  $f_c = 2eV_c/h = 71$  GHz calculated from  $V_c = I_c R_N = 147 \mu\text{V}$  (static estimation of  $f_c$ ) and the  $f_c = 56$  GHz determined from the maximum value of the first Shapiro step using the RSJ model approach (dynamic  $f_c$ ) [10].

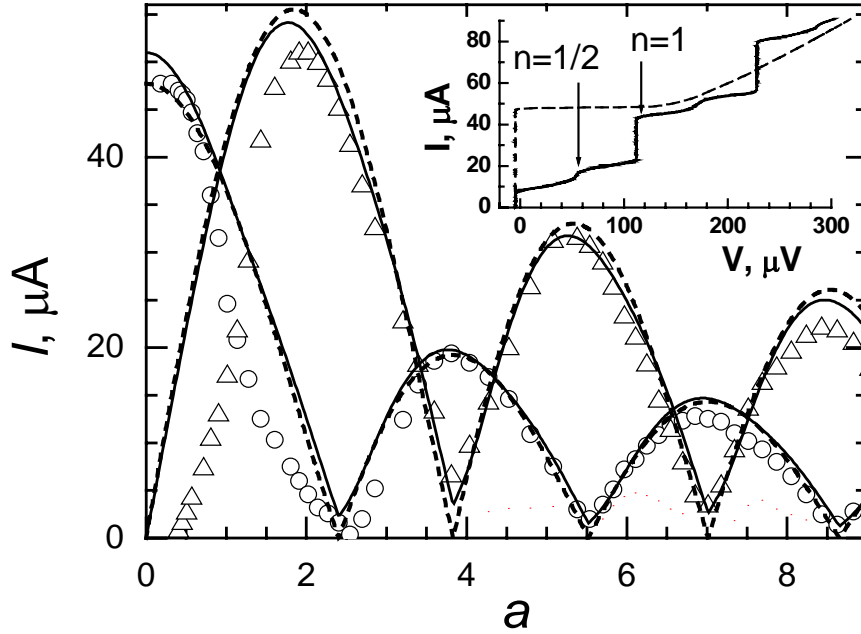


Fig. 6. The critical current  $I_c$  (circles) and first Shapiro step  $I_1$  (triangles) vs normalized  $a=I_e/I_c$  microwave current  $I_e$  at  $T=4.2$  K, microwave frequency  $f_e=56$  GHz. The solid lines correspond to the  $I_c(a)$  and  $I_1(a)$  curves numerically calculated from the modified RSJ model taking into account the second harmonic in CPR for  $q=0.2$ , dashes - for  $q=0$ . The  $I-V$  curves with (solid line) and without (dashes) external microwaves are shown in the inset. Positions of integer  $V_1=nhf_e/2e$  ( $n=1$ ) and half-integer  $n=1/2$  Shapiro steps are indicated by arrows.

The deviation of experiment from model calculations becomes smaller if we take into account a presence of the second harmonic component in the CPR, which is manifested by fractional Shapiro steps (inset Fig. 6) observed at all experimental frequencies up to 120 GHz. At the same time it is known, that fractional Shapiro steps may originate also from the finite capacitance  $C$  of the Josephson junction (McCumber  $\beta_c=(2e/\hbar)I_cR_N^2C>1$ ) [9]. We estimated  $\beta_c=2\div 6$  from the hysteretic  $I-V$  curves. In order to investigate the influence of the second harmonic in the CPR and the capacitance  $C$  on dynamics of MHS we have studied dependences of the critical current  $I_c(a)$  and the first Shapiro step  $I_1(a)$  vs. normalized amplitude  $a=I_e/I_c$  of external microwave current  $I_e$ . Amplitudes  $a$  were determined [9, 10] from the attenuation levels of applied microwave power. The performed calculations of the Shapiro step amplitudes based on the modified RSJ model (taking into account the  $\beta_c$  parameter) show that at frequencies  $f_e>f_c$  the impact of capacitance  $C$  on Shapiro steps amplitudes is small, and the  $I_c(a)$  and  $I_1(a)$  dependences are determined mainly by the first and the second harmonics of the CPR. The experimental data presented in Fig. 6 are fitted well to the theoretical dependencies calculated taking into account the amplitude  $I_{c2}$  of the second harmonic in the CPR  $q=I_{c2}/I_c=0.2$ . Note the sign of  $q$  can be determined by analyzing the experimental dependence of half integer Shapiro step  $I_{1/2}(a)$  in comparison with the theoretical calculated one [9]. This procedure gives us negative  $q<0$ . The presence of the second harmonic in the CPR of the MHS indicates an existence of a portion of d-wave component in M-interlayer.

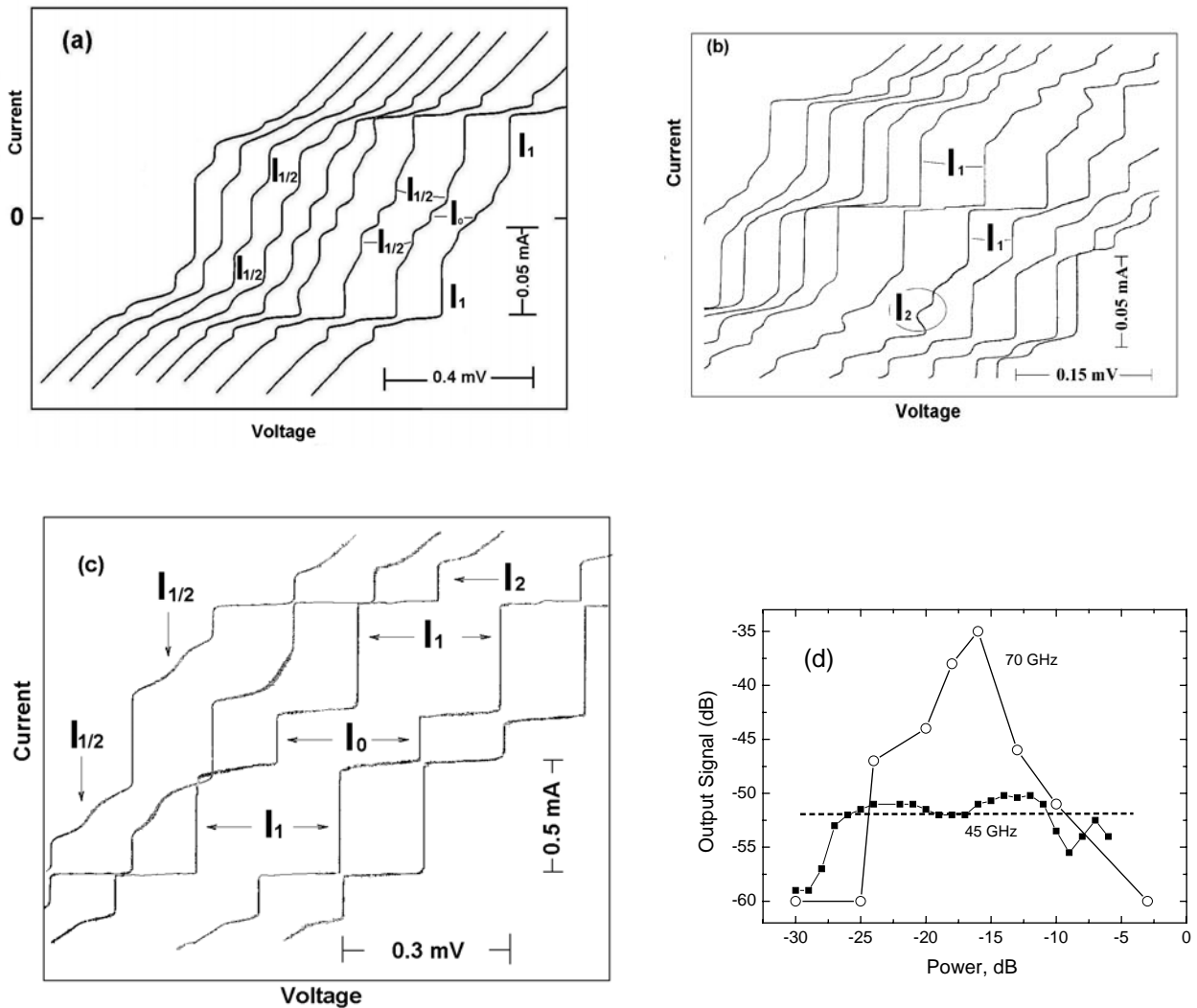


Figure 7. Families of  $I$ - $V$  curves under different power levels of microwave irradiation  $f=45$  GHz (a, b) and  $f=70$  GHz (c). Critical current  $I_C$ , integer  $I_1$ ,  $I_2$  and half-integer  $I_{1/2}$  Shapiro steps are indicated. (b):  $n=2$  Shapiro step distortion is pointed by circle. (c): Chaotic noise rise corresponds to the jerks on  $I_{1/2}$  steps. All curves are shifted by voltage to the right with increase of applied power. AF interlayer was  $\text{Ca}_{0.5}\text{Sr}_{0.5}\text{CuO}_2$ , dimensions  $20 \times 20 \mu\text{m}$ ,  $d=20$  nm,  $I_C=55 \mu\text{A}$ ,  $R_N=5.5 \Omega$ , and  $\beta_C=2$ . (d): Output signal measured in 1-2 GHz frequency band under microwave power  $P$  at 45 GHz (black symbols) and 70 GHz (open symbols). Dash line shows saturation level for frequency mixing.

For a junction with  $c$ -oriented YBCO film a “devil” staircase structure on  $I$ - $V$  curve was observed under microwave irradiation at 45 GHz. Fig. 7 shows such  $I$ - $V$  curves evolution when applied power was changed. Distortion of the 2<sup>nd</sup> Shapiro step is seen at large power levels (Fig. 7b) observed within narrow attenuation range  $\alpha=3$  dB. Fig. 7a demonstrates unusually large half-integer  $n=1/2$  Shapiro steps: up to 0.4 of critical current  $I_C$ . That could be caused by superposition of two processes, first one is due to existence of the second harmonic in current-phase relation, and the second one could be related to the period doubling under the large microwave signal when frequency of applied signal  $f_e$  is not far from plasma frequency of Josephson junction  $f_p=(2eI_C/hC)^{1/2}$ , where  $e$  is electron charge,  $h$  is Planck’s constant. Fig. 7c shows  $I$ - $V$  curves with the jerks at biasing voltages between integer Shapiro steps when 70 GHz signal was applied and a giant noise rise was registered by cooled amplifier within 1-2 GHz band. Note, power of applied signal was large enough and a frequency mixing effect also takes place due to existence of self-Josephson radiation. In order to compare intensities of the frequency mixing products with the chaotic oscillations we estimated the output signal saturation in frequency mixing regime. Fig. 7d shows the dependences of output signal levels vs.

applied power of microwave signals at  $f_e = 45$  GHz and 70 GHz when current bias was fixed, keeping the voltage near the half-integer Shapiro step  $V_{1/2} = (2e/h)/f_e$ , where chaotic behaviour was observed. The output signal saturation level in frequency mixing process is also shown. Experimental conditions for chaotic oscillations in Josephson junctions were analysed [11] and were experimentally observed [12] in the case of superconducting tunnel junctions with  $\beta_C > 25$ . However, our junctions had relatively small  $\beta_C$  parameters. Recently chaotic dynamics was predicted [13] for S/F/S Josephson structures with magnetic interlayer consisted of 3 separated F-layers with rotated magnetization. Although we did not obtain experimental evidence for the triplet Josephson effect in our structures, the latter finding points on very complicated high frequency dynamics in Josephson junctions with magnetic interlayer. These results show that along with the search for promising materials of magnetic interlayer aiming at applications at microwaves the dynamics of such junctions with magnetic interlayer should be studied in details in order to avoid chaotic behaviour and unstable operation.

#### 4. Conclusions

Hybrid superconducting Josephson junctions with an antiferromagnetic  $d=10 - 50$  nm thick interlayer were fabricated on NdGaO<sub>3</sub> substrates. Exponential decrease of critical current density with AF layer thickness was observed. Superposition of magnetic and microwave fields did not lead to distortion in symmetry of  $I-V$  curves: equal Shapiro step amplitudes were registered at positive and negative voltage biasing. The sensitivity to applied magnetic field for these junctions was found much higher than for conventional Josephson junctions. Then, half integer Shapiro steps observed along with the sub-harmonic frequency selective detector response. That points on deviation of current-phase relation from sinusoidal one. At the same time at the certain experimental conditions a “devil” staircase appears on  $I-V$  curves and the giant noise-like signal was registered for the junction fabricated using  $c$ -oriented YBCO electrode.

#### Acknowledgment

This work was supported by Russian Academy of Sciences, Scientific School Grant 5423.2010.2, Russian Ministry of Education and Science - contract 02.740.11.0795, RFBR proj. 08-02-00487, ISTC proj. 3743.

#### References

- [1]. A.I. Buzdin. Rev. Mod. Phys. **77** (2005) 935.
- [2] F.S. Bergeret, A.F. Volkov, K.B. Efetov. Rev. Mod. Phys. **77** (2005) 1321.
- [3] L. Gor'kov, V. Kresin. Appl. Phys. Lett. **78**, 3657 (2001), Physics Reports **400** (2004) 149.
- [4]. A.V. Zaitsev. JETP Lett. **90** (2009) 521.
- [5]. C. Bell, E.J. Tarte, G. Burnell, C.W. Leung, D.-J. Kang, and M.G. Blamire. Phys. Rev. **B68**, (2003) 144517.
- [6]. P.V. Komissinskiy, G.A. Ovsyannikov, I.V. Borisenko, Yu.V. Kislinskii, K.Y. Constantinian, A.V. Zaitsev, D. Winkler. Phys. Rev. Lett. **99** (2007) 017004.
- [7]. Y.V. Kislinskii, K.Y. Constantinian, G.A. Ovsyannikov, P.V. Komissinskiy, I.V. Borisenko, A.V. Shadrin. JETP **106** (2008) 800.
- [8]. A.V. Zaitsev, G.A. Ovsyannikov, K.Y. Constantinian, Y.V. Kislinskii, A.V. Shadrin, I.V. Borisenko, P.V. Komissinskiy. JETP **110** (2010) 336.
- [9]. P. V. Komissinskiy, G. A. Ovsyannikov, K.Y. Constantinian, Y.V. Kislinski, I.V. Borisenko, I.I. Soloviev, V.K. Kornev, E. Goldobin, and D. Winkler. Phys. Rev. **B78** (2008) 024501.
- [10]. A. Barone, G. Paterno (N.-Y. Awaley-Interscience Publication John Wiley and Sons, 1982).
- [11]. R. Kautz, R. Monaco. J. Appl. Phys. **57** (1985) 875.
- [12]. Gubankov V.N., Constantinian K.Y, Koshelets V.P., Ovsyannikov G.A., Vystavkin A.N. IEEE Tr. on MAG-19 (1983) 968.
- [13] V. Braude and Ya.M. Blanter. Phys. Rev. Lett **100** (2008) 207001.